Materials Today Communications 23 (2020) 100884

Contents lists available at ScienceDirect

Materials Today Communications

journal homepage: www.elsevier.com/locate/mtcomm

Synergistic and enhanced anticancer effect of a facile surface modified non-cytotoxic silver nanoparticle conjugated with gemcitabine in metastatic breast cancer cells

Arjunan Karuppaiah[a,1], Karthik Siram[a,b], Divakar Selvaraj[c,d], Mohankandhasamy Ramasamy[e], Dinesh Babu[f], Veintramuthu Sankar[a,*]

[a] Department of Pharmaceutics, PSG College of Pharmacy, Coimbatore 641 004, Tamil Nadu, India
[b] Institute of Plant Genetics, Polish Academy of Sciences, Strzeszynska 34, 60-479, Poznan, Poland
[c] Department of Pharmacology, PSG College of Pharmacy, Coimbatore, Tamil Nadu, India
[d] Department of Pharmacology, JSS College of Pharmacy, JSS Academy of Higher Education and Research, Ooty, Nilgiris, Tamil Nadu, India
[e] Department of Chemical Engineering, Waterloo Institute of Nanotechnology, University of Waterloo, Waterloo, N2L 5G1, Canada
[f] Faculty of Pharmacy and Pharmaceutical Sciences, Katz Group Centre for Pharmacy and Health Research, University of Alberta, Edmonton, Alberta, T6G 2R3, Canada

ARTICLE INFO

Keywords:
Breast cancer
Gemcitabine
Silver nanoparticles
Synergism
Electrostatic attraction

ABSTRACT

The safety and efficacy of metallic nanoparticles was one of the major challenges that limit their use in the treatment of cancer. Nanotechnology is applied in the field of pharmaceutical sciences with focus on improving the therapeutic outcome in various diseases. Recently, many novel nano-formulations comprising two or more drugs were studied to improve their efficacy with better safety profile. In this study, we investigated the synergistic cytotoxic effect of gemcitabine (GEM) conjugated non-cytotoxic dose of silver nanoparticles (AgNP) in MDA-MB-453 human triple-negative metastatic breast cancer cells. Synthesized AgNP and electrostatic conjugates were characterized by UV-spectroscopy, dynamic light scattering (DLS), Transmission electron microscopy (TEM), Scanning electron microscopy (SEM) and energy dispersive x-ray analysis (EDAX). GEM-(non-cytotoxic AgNP) conjugated system (IC_{50} = 37.64 μM) showed better cytotoxic activity in MDA-MB-453 cells when compared to individual treatments of GEM (IC_{50} = 56.54 μM) or AgNP (IC_{50} = 71.45 μg/ml). The synergism between the GEM-(non-cytotoxic AgNP) for all the tested doses were evaluated using CompuSyn software. The combination index (CI) of ED_{50}, ED_{75} and ED_{90} showed synergism for GEM-(non-cytotoxic AgNP) conjugation. According to the calculated dose reduction index (DRI), it requires 1.70-fold less GEM plus 42.55-fold less AgNP to achieve the same 50 % inhibition at 18.38 (GEM): 1 (AgNP) ratio.

1. Introduction

Nanotechnology is applied in various fields of pharmaceutical sciences to improve the physicochemical and ADME properties, efficacy and safety of the drugs [1]. One such approach is combining effective metallic nanoparticles with chemotherapeutic agents [2]. Metallic nanoparticles possess unique properties due to their size, shape, surface structure and aggregation characteristics [3]. Amongst, AgNP is the one which is extensively studied in pharmaceutical sciences because of its antimicrobial activity and cytotoxicity against various cancer cell lines [4–6]. Nano silver can be easily oxidized in the presence of oxygen leading to the release of silver ions (Ag^+) which is the major source of toxicity. Thus, AgNP often acts as a source of Ag^+ inside the cells. Ag^+ ions induce oxidative stress through the generation of reactive oxygen species and causes damage to cellular components such as cell membrane, protein and DNA. This leads to apoptotic and necrotic cell deaths triggering the release of pro-inflammatory cytokines which cause further damage to nearby tissues or cells. AgNP can also deplete the antioxidant molecules like glutathione and aggravate the cytotoxic effects. AgNP are reported to cause genotoxicity, neurotoxicity, pulmonary toxicity, hepatotoxicity and immunotoxicity [7]. Necropsy analysis of rats orally administered with AgNP (5 mg/kg b.w. and 10 mg/kg b.w.) for 28 days showed no signs of toxicity in the organs such as kidney, brain, lungs, heart and testis. Liver cells had some anomaly in 10 mg/kg b.w. treatment and not in 5 mg/kg b.w. treated rats [8]. Hepatoma cells (HepG2) treated with non-cytotoxic dose (< 0.5 mg/L) of AgNP

* Corresponding author.
E-mail address: sansunv@yahoo.co.in (V. Sankar).
[1] Affiliated to TN Dr M.G.R Medical University, Guindy, Chennai 600032, Tamil Nadu, India.

https://doi.org/10.1016/j.mtcomm.2019.100884
Received 22 August 2019; Received in revised form 26 December 2019; Accepted 28 December 2019
Available online 30 December 2019

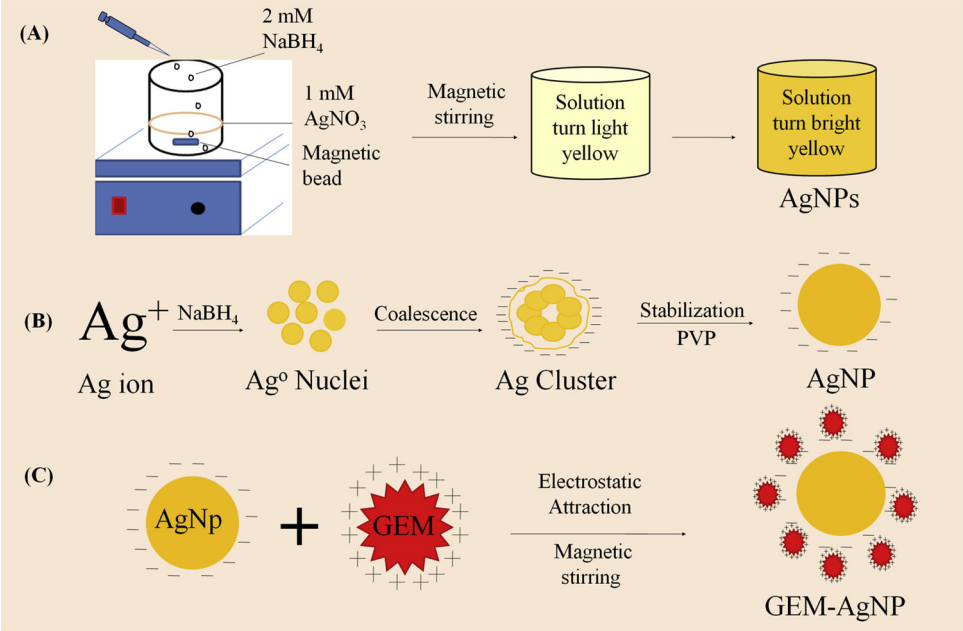

Fig. 1. Schematic representation: (A) Synthesis of AgNP, (B) Mechanism of AgNP formation and stabilization using PVP, and (C) Surface adsorption of GEM on AgNP.

exhibited protective effect. The toxic effects were observed only in the doses excess of 1 mg/l in HepG2 cells [9]. Moreover, the protective effect of AgNP at low doses was correlated with its ability to activate Nrf2 (nuclear factor erythroid 2(NFE2)-related factor 2) and P38 MAPK mediated transcriptional process. Hence, reducing the dose of AgNP is a prime prerequisite to minimize toxicity associated with AgNP usage to treat disease conditions [10].

Monotherapy for cancer treatment has many drawbacks such as drug resistance, excessive toxic effects and undesired side effects. The advantage of combination therapy includes the use of chemotherapeutic agents and NP at lower doses. This could result in the elimination/reduction of undesired toxic effects and increased efficacy. In practice, combination chemotherapy results in better response and improved survival compared with single-agent therapy [11]. Metastatic breast cancer is often treated with combinations such as cyclophosphamide / doxorubicin / fluorouracil, cyclophosphamide / doxorubicin, cyclophosphamide / methotrexate / fluorouracil, gemcitabine / paclitaxel and gemcitabine / carboplatin [12]. However, many chemotherapeutic drugs have systemic toxicity because they non-specifically accumulate in normal cells [13]. Hence, improving the safety and synergy of chemotherpeutic agents in monotherapy is the need of the hour to treat cancer. The dose limitation of AgNP could be achieved by combining a proper cytotoxic drug to exploit the synergism between the two agents [14]. Hence, in this study, we controlled the ratio and tested the synergistic effect of non-cytotoxic dose of AgNP conjugated with a cytotoxic agent gemcitabine (GEM). Synthesis of AgNP generally involves reducing the precursor Ag^+ by techniques such as biological, chemical, electrochemical reduction and radiolysis. Among them, size controllable chemical reduction is the most popular to get uniform AgNP using chemical reductants such as sodium citrate [15], tannic acid [16], sodium borohydride ($NaBH_4$) [17], hydrazine [18] and hydroxylamine hydrochloride [19]. Generally, AgNP have stability issues such as aggregation, crystal growth and poor size distribution. After stabilization, chemically reduced AgNP are reported to be highly stable at room temperature (23 °C) over a period of one year when compared to bare AgNP [20].

AgNP with different surface charges can be synthesized using different types of reducing agents. To obtain AgNP with negative, neutral and positive surface charge, $NaBH_4$, rice starch and 1-dodecyl-3-methylimidazolium chloride were used, respectively [21–23]. During the synthesis of nanoparticles, the ligand molecules bound to the surface prevent the growth and aggregation of nanoparticles. The ligand molecules bind to the surface of the particles by attractive interactions such as chemisorption, electrostatic attraction and hydrophobic interactions [24–26]. Electrostatic attraction of ligands on metallic nanoparticles has been widely studied. Metallic nanoparticle system such as folic acid-conjugated AgNP, polymyxin B-conjugated gold nanoparticles and pyrethroid-conjugated on nanosilver have been previously studied [2,27–29]. Surface functionalization of AgNP is important for their applicability, compatibility and safety. AgNP act as a drug carrier with enhanced stability of surface adsorbed drug. It has diagnostic potency, enhanced catalytic activity, reduced toxicity, and high-density surface for ligand attachment without additional use of any linkers and protects the surface attached drug from degradation. Surface functionalization defines how nanoparticles behave in physiological conditions [30,31]. In this study, we developed a system with AgNP as a core which is electrostatically attached to GEM. This system was evaluated in human triple-negative metastatic breast cancer cell line, MDA-MB-453.

2. Materials and methods

2.1. Materials

GEM (as gemcitabine hydrochloride) was a gift sample from Dr. Reddy's Laboratories, Hyderabad, India. Silver nitrate ($AgNO_3$), $NaBH_4$, polyvinyl pyrrolidone (PVP), sucrose and sodium chloride (NaCl) were purchased from Sigma Aldrich, India. MDA-MB-453 was purchased from National Centre for Cell Science (NCCS), Pune, India.

2.2. Synthesis of AgNP

AgNP were synthesized by chemical reduction method using $NaBH_4$ as a reducing agent [21]. Briefly, 10 ml of 1.0 mM $AgNO_3$ solution was added drop wise to 30 ml of 2.0 mM ice-cold $NaBH_4$ solution. The reaction mixture was stirred on a magnetic stirrer until a color change was obtained (Fig. 1A). Formation of bright yellow color indicates the successful formation of AgNP. During the reaction, AgNP can get aggregated and this leads to the conversion of bright yellow to grayish color solution.

2.3. Stabilization of AgNP

Further, the colloidal AgNP were stabilized using PVP to prevent from the aggregation (Fig. 1B). Typically, 0.5 ml aqueous solution of PVP (0.3 %) was added to 40 ml of AgNP and the reaction mixture was stirred on a magnetic stirrer for 10 min, and free Ag^+ were separated by ultracentrifugation at 13,000 rpm for 45 min [17].

2.4. Freeze-drying of AgNP

Freeze-drying is a process used for drying and to improve the stability of nanoparticles. 1 % sucrose was used as a cryoprotectant. Sucrose solution was added drop by drop to AgNP solution under magnetic stirring. The mixture was kept at -80 °C for 24 h to solidify and the sample was kept in a freeze dryer (LYODEL, Chennai, India) for 24 h [32].

2.5. Adsorption of GEM on AgNP

GEM is adsorbed to AgNP surface by electrostatic interaction method which is a non-covalent bond occurring between two oppositely charged particles. GEM 10 mg was added to 5 ml (1.37 mg of freeze-dried) of AgNP colloidal solution, and stirred in a magnetic stirrer at room temperature for 24 h (Fig. 1C). The solution was centrifuged at 10,000 rpm for 15 min to collect GEM-AgNP conjugate. The concentration of free-GEM present in the supernatant was determined using UV-spectroscopy at 268 nm. The amount of drug adsorption and the adsorption efficiency were calculated according to the formulae given below (Formula 1 and 2) [33]. The pH of the AgNP and GEM-conjugated AgNP was measured using Systronics μ pH System 361 (Ahmedabad, India).

$$\text{Amount of drug adsorbed} = \text{Initial drug loaded} - \text{Unabsorbed drug} \quad (1)$$

$$\text{Adsorption efficiency (\%)} = \left[\frac{\text{Amount of drug adsorbed}}{\text{Initial drug loaded}}\right] \times 100 \quad (2)$$

2.6. Characterizations of AgNP

The surface plasmon resonance of AgNP was carried out using UV-spectroscopy (UV-1601 PC Shimadzu Spectrophotometer, Japan). The λ_{max} was measured at the wavelength ranging from 300 to 800 nm. The mean diameter and zeta potential of AgNP were measured by dynamic light scattering (DLS) using Zetasizer (Nano ZS 90, Malvern Instruments, United Kingdom). Transmission electron microscopy (TEM 120 kV; T12 Fei, Tecnai G2 Sprit TWIN) and scanning electron microscopy (SEM; Zeiss Sigma, Germany) were performed to analyze the morphology of the AgNP. Energy dispersive x-ray analysis (EDAX) (T12 Fei, Tecnai G2 Sprit TWIN) observation was carried out to find the elements present in the formulation and to confirm their electrostatic attraction. The EDAX spectrum of AgNP was recorded in the spot profile mode from one of the densely populated regions on the surface of the grid.

2.7. In-vitro drug release study

In-vitro drug release of GEM and GEM-AgNP was carried out for 24 h in phosphate buffered solution (PBS) at pH 7.4. Typically, 3 mg/ml of GEM and GEM-AgNP was placed in a dialysis bag and suspended in 50 ml of PBS at 37 °C under gentle magnetic stirring (100 rpm). At a fixed time interval, 2 ml of buffer medium was withdrawn and replaced with an equal volume of fresh medium. The amount of GEM released at a fixed time interval (0, 0.5, 1, 2, 4, 6, 12 and 24 h) was estimated by UV-Spectrophotometry (268 nm, UV-1601 PC Shimadzu Spectrophotometer, Japan). The cumulative release percentage of GEM at each time point was determined.

2.8. Stability study

In order to check the stability of the synthesized colloidal solution, AgNP was aliquoted into two well closed containers and kept at 4.0 ± 2.0 °C and 23.0 ± 2.0 °C, respectively. The UV–vis and DLS measurements were carried out periodically to observe the changes in the colloidal AgNP solution [34].

2.9. In-vitro cell studies

MDA-MB-453 cells were cultured in Roswell Park Memorial Institute (RPMI) medium supplemented with 10 % fetal bovine serum (FBS), 1 mM sodium pyruvate and 2 mM glutamine. The cells were cultured in a cell culture incubator at 37 °C with 5 % CO_2. *In vitro* cytotoxicity of GEM, AgNP and GEM-AgNP was tested using 3-(4,5-dimethylthiazol-2-yl)-2,5-diphenyltetrazolium bromide (MTT) assay. Briefly, the cells were seeded in 96-well plates at the density of 3000 cells/well. After 24 h, the existing media was removed and replaced by fresh media along with various concentrations of the prepared drug and nano formulations (1.56, 3.12, 6.25, 12.5, 25, 50, 75 and 100 μM and μg/ml for GEM and AgNP, respectively). The cytotoxicity of GEM-AgNP was evaluated at the following concentrations 1.56 + 0.08, 3.12 + 0.17, 6.25 + 0.34, 12.50 + 0.68, 25 + 1.36, 50 + 2.72, 75 + 4.08 and 100 + 5.45 (μM GEM + μg/ml AgNP). The cells were incubated for 48 h and the medium was replaced with fresh medium containing 10 μl of MTT solution (5 mg/ml) in each well and incubated for another 4 h. Then, the formazan crystals were dissolved using 100 μl of DMSO and the optical density was measured at 570 nm in a microplate reader (Thermo Scientific, Multiskan GO Microplate Spectrophotometer, Finland). The cytotoxicity was calculated using the formula mentioned below (Formula 3). The IC_{50} was calculated by constructing a dose-response curve using GraphPad Prism software version 5.

$$100 - \left(\frac{\text{At} - \text{Ab}}{\text{Ac} - \text{Ab}}\right) \times 100 \quad (3)$$

where, At- absorbance of test drug
Ab- absorbance of blank
Ac- absorbance of control

2.10. Combination index

The synergistic cytotoxic effect of GEM-AgNP on triple negative breast cancer cells was evaluated using CompuSyn software. The GEM-AgNP formulation was prepared with constant combination ratio between GEM and AgNP. The cytotoxicity of GEM-AgNP was evaluated at the following concentrations 1.56 + 0.08, 3.12 + 0.17, 6.25 + 0.34, 12.50 + 0.68, 25 + 1.36, 50 + 2.72, 75 + 4.08 and 100 + 5.45 (μM GEM + μg/ml AgNP) where a constant ratio of 18.32:1 (GEM:AgNP) was maintained. The cytotoxicity was determined by MTT assay as described in earlier section. The CompuSyn software calculates the combination index (CI) value by median effect principle. This software is based on Chou and Talalay's multiple drug effect equations. The following equation is used to calculate the CI (Formula 4).

$$CI = (D)_1/(Dx)_1 + (D)_2/(Dx)_2 \quad (4)$$

In the equation, $(Dx)_1$ and $(Dx)_2$ indicates the individual dose of GEM and AgNP that required to inhibit the prescribed level of cell growth. The $(D)_1$ and $(D)_2$ are the doses of individual drugs necessary to produce the equal effect in combination. Combination index (CI) value < 1, = 1 and > 1 indicate synergism, additive effect and antagonism, respectively [35].

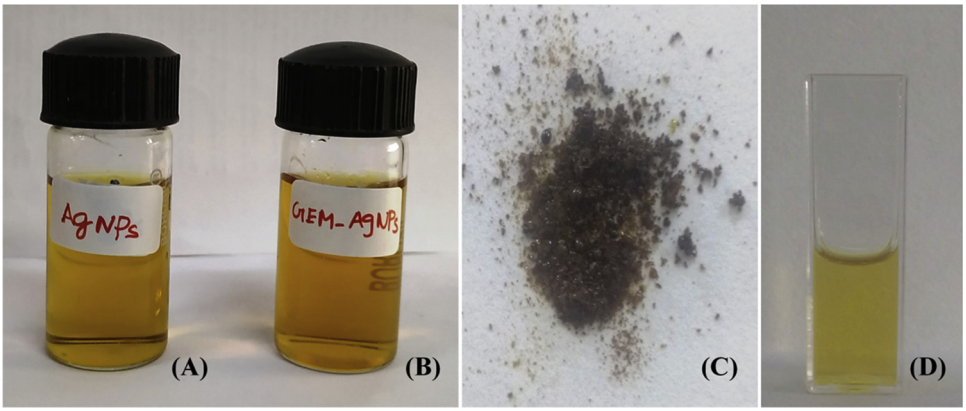

Fig. 2. (A) AgNP, (B) GEM-AgNP, (C) Freeze-dried AgNP, and (D) Dispersion of freeze-dried AgNP in water.

2.11. Statistical analyses of data

Statistical analyses were performed using Prism software (Version 5, GraphPad, GraphPad Software Inc., La Jolla, CA, USA). Results are expressed as the mean of three replicates ± standard deviation (SD). A level of statistical significance between groups was analyzed by unpaired *t*-test. $P < 0.05$ was considered statistically significant.

3. Results and discussion

AgNP were prepared from $AgNO_3$ by chemical reduction method with the indication of nanoparticle formation by bright yellow color and the addition of GEM did not result in any color transition (Fig. 2A and B). Prepared AgNP were stabilized using 0.3 % PVP (w/v). PVP is a polymer which has been reported to be strongly adhere to the surface of AgNP, preventing aggregation and enhances the stability of AgNP for over a year [21,36]. The synthesized AgNP were added with sucrose as a cryoprotectant to immobilize the nanoparticles within a glassy matrix to protect them from aggregation during freeze drying. The freeze-drying of 40 ml of prepared colloidal AgNP yielded 11 mg of coarse powder (Fig. 2C). The freeze-dried powder was redispersed in distilled water and used for further characterizations and *in vitro* assays (Fig. 2D). The adsorption of GEM on AgNP was studied at 25 °C temperature. The adsorption efficiency was found to be 75.6 % and the prepared formulation was used for *in vitro* assay. Due to smaller particle size and higher surface area, AgNP can bind to different molecules. A drug surface functionalized nanoparticle has higher blood circulation in the body than the un-adsorbed nanoparticles. The drug adsorbed nanoparticles have lower lymph drainage and higher accumulation at the tumor site and exerts increased toxicity to the cancerous cells than with the drug alone [37].

The pH of AgNP was initially 8.9 which was reduced to acidic pH 3.1 after the adsorption of GEM (Table 1). The pH of the solution plays a key role to facilitate electrostatic attraction between the charged metallic nanoparticles and the drug. Acidic pH values are due to the electrostatic attraction between the metallic nanoparticles and the drug [38]. In this study, a pH value of 3.1 was obtained for GEM-AgNP, which indicated a strong electrostatic attraction between GEM and AgNP.

The resonance wavelength of AgNP depends on particle size and shape. If the particle size becomes larger, the plasmon peak shifts to longer wavelengths and broadens [33]. AgNP has a strong absorption peak close to 390 nm and this confirms that the Ag^+ was reduced to AgNP [36]. The UV-spectra of the colloidal AgNP and GEM-AgNP has single plasmon absorption peak (Fig. 3) at 395 ± 0.28 and 411 ± 0.57 nm, respectively. A red shift in the plasmon absorption peak of AgNP was observed which confirms the surface modification of the NP by successful adsorption of GEM (Table 1 & Fig. 3). The pH changes do not affect the intensity of the bands formed by GEM and AgNP separately, and this indicates that there are no aggregations in GEM-AgNP solution.

The average particle size of AgNP and GEM-AgNP was found to be 9.16 ± 0.28 and 19.06 ± 0.50 nm, respectively (Table 1) ($p < 0.0001$). The particle size of GEM-AgNP was higher than AgNP because of the adsorption of GEM to AgNP. However, there was no evidence of aggregation and morphological changes in GEM-AgNP. The Poly Dispersive Index (PDI) of AgNP and GEM-AgNP was found to be 0.325 ± 0.05 and 0.307 ± 0.05, respectively. This indicates that the particles were homogeneous ($p < 0.0004$) [39]. The electrophoretic property of AgNP and GEM-AgNP was determined by measuring the zeta potential. The zeta potential of AgNP and GEM-AgNP was found to be - 46 ± 0.25 and -30.3 ± 0.20 mV, respectively ($p < 0.0010$) (Table 1). A change in surface potential was observed after the addition of GEM to AgNP, which was due to the electrostatic attraction between the negatively charged AgNP and positively charged GEM. The zeta potential of the system should be higher than +30 mV or lower than −30 mV to resist aggregation [40]. SEM and TEM micrographs of AgNP and GEM-AgNP indicate that the formed particles are spherical and monodispersed with a particle size less than 25 nm (Figs. S1A & Fig. 4A). No change in the morphology after the adsorption of GEM to AgNP was observed in SEM and TEM micrographs (Figs. S1B & 4B). The particle size was in agreement with the values obtained by DLS. The images of GEM-AgNP clearly showed that the formed and surface modified AgNP were free of aggregations.

EDAX gives qualitative status of elements that may be involved in the formation of AgNP. The EDAX of AgNP showed signature peaks for silver (Ag), copper (Cu) and carbon (C) (Fig. 4C). The peaks for Cu and C were also observed because of the carbon grid that was used to prepare the sample whereas, EDAX of GEM-AgNP shows the signature peaks of both Ag and GEM ($C_9H_{12}ClF_2N_3O_4$) (Fig. 4D). The EDAX peaks

Table 1
Physicochemical characterizations of bare and surface-modified AgNP.

Formulations	Average Particle Size (d. nm)	Zeta Potential (mV)	PDI	UV-Plasmon Peak (nm)	pH
AgNP	9.16 ± 0.28	−46.7 ± 0.25	0.325 ± 0.05	395 ± 0.28	8.9 ± 0.10
GEM-AgNP	19.06 ± 0.50	−30.3 ± 0.20	0.307 ± 0.05	411 ± 0.57	3.1 ± 0.20

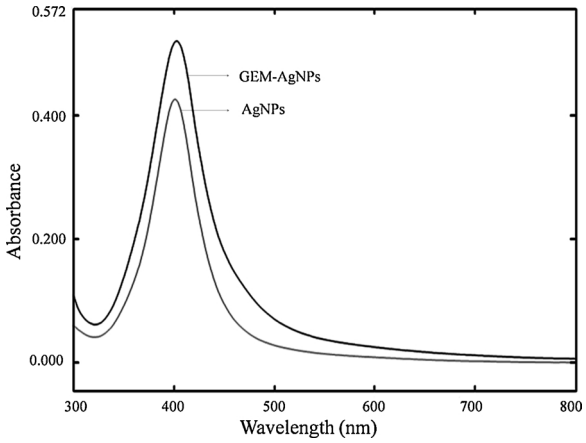

Fig. 3. Plasmon resonance peak of AgNP and GEM-AgNP.

of functional elements such as Ag, fluorine (F), nitrogen (N) and chlorine (Cl) were observed in the GEM-AgNP formulation, which confirm the conjugation of GEM to AgNP [41].

The *in-vitro* cumulative percentage release of GEM solution and GEM-AgNP in PBS pH 7.4 is shown in Fig. 5. The GEM alone had undergone burst release of 92.5 ± 1.75 % within 4 h and shown 98.9 ± 1.53 % release at the end of 24th h. On the other hand, GEM-AgNP also had undergone burst release of 87 ± 1.52 % within 4 h and shown 91.5 ± 1.45 % release at the end of 24th h (Table S1). GEM alone shown maximum drug release at the end of 24 h when compared to GEM-AgNP; however, both the GEM and GEM-AgNP shown burst release until 0.5–4 h. Typically, electrostatic interaction or physical adsorption (by non-covalent interaction) shows weak bonding and will

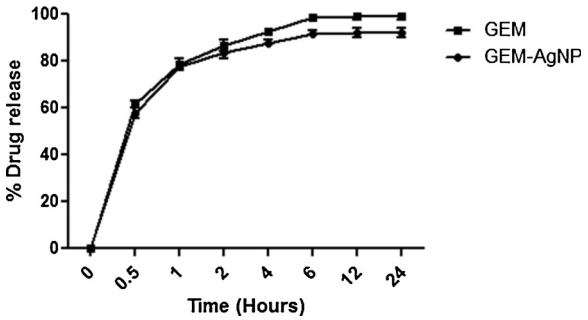

Fig. 5. The *in-vitro* cumulative percentage release of GEM solution and GEM-AgNP in phosphate buffer solution pH 7.4.

not be strong like covalent bond [42]. In our formulation, GEM is adsorbed on the AgNP surface by electrostatic affinity; when this conjugate reaches the aqueous medium, the drug will start to dissociate and dissolve like free drug (GEM).

Generally, nanoparticles have poor long-term stability due to different physical and chemical factors that may destabilize the system, so, the UV-absorbance was recorded periodically during the stability study (Table S2). We observed that the absorbance of the formulations stored at 23.0 ± 2.0 °C increased over time (Fig. 6A & C). But, the absorbance of the formulation stored at 4.0 ± 2.0 °C remained stable [33], which indicated that the formulation showed a good stability at 4.0 ± 2.0 °C (Fig. 6B & D). The particle size, PDI and zeta potential were increased at room temperature but the values of these parameters of the formulations remained stable at 4.0 ± 2.0 °C (Table S2). However, both the storage conditions did not result in aggregation or colour changes of the formulation. AgNP are susceptible to oxidation so storing them at refrigerator temperature in dark mode can protect them from light, and

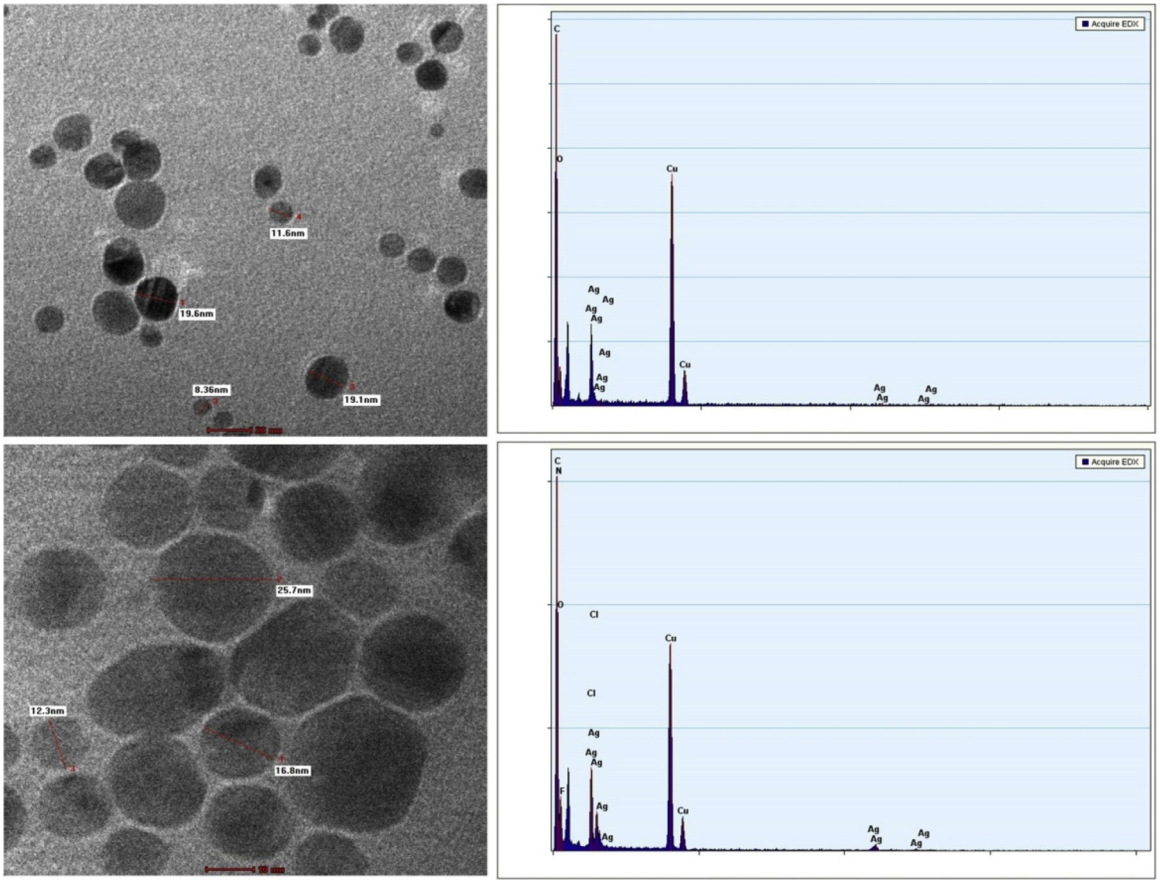

Fig. 4. (A) TEM images of AgNP and (B) TEM images of GEM-AgNP (C) EDAX Spectra of AgNP and (D) EDAX Spectra of GEM-AgNP.

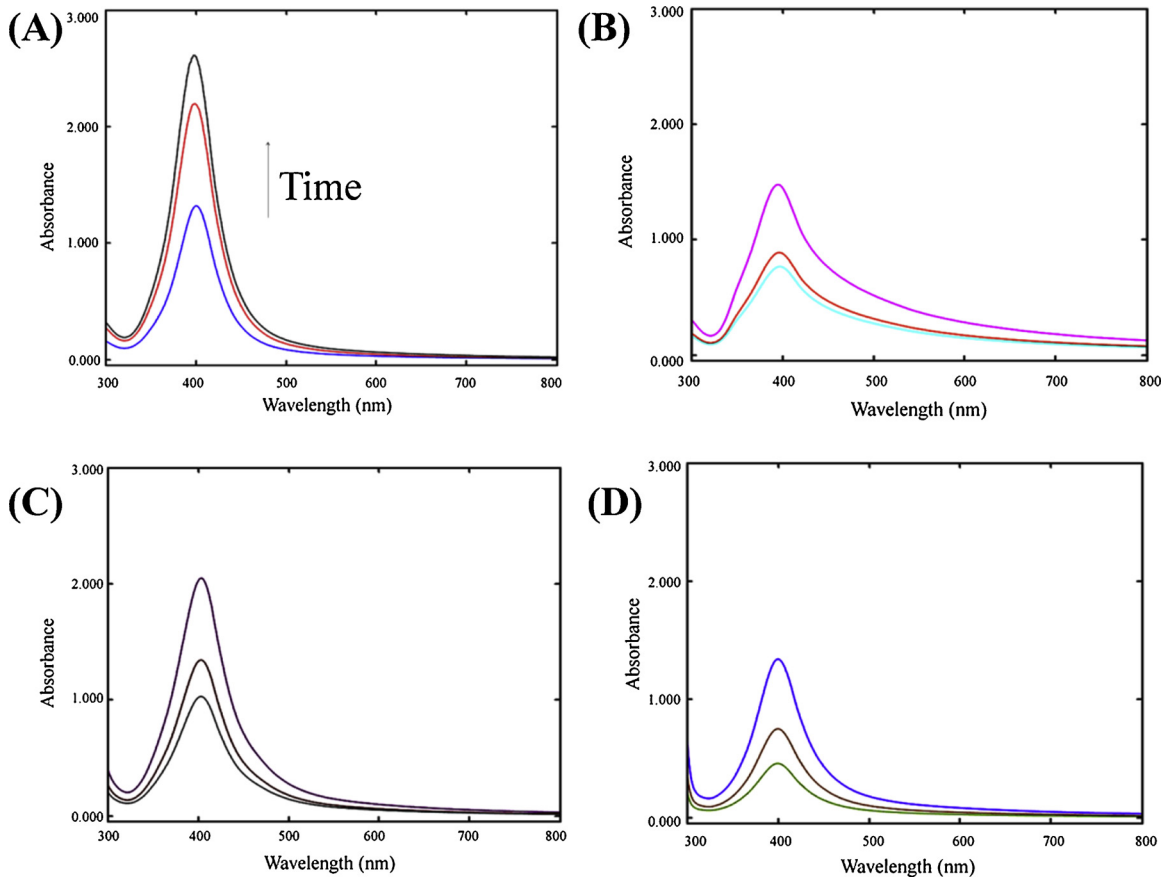

Fig. 6. UV-plasmon absorbance at different time intervals and temperatures (A) AgNP at room temperature, (B) AgNP at refrigerator temperature, (C) GEM-AgNP at room temperature, and (D) GEM-AgNP at refrigerator temperature.

this may be the reason for slight physicochemical changes of AgNP when stored at room temperature.

The toxicity of AgNP is the major limiting factor for its *in-vivo* use [43] and has been proved to cause mitochondrial toxicity on repeated doses and lead to the damage of major organ systems [44]. The toxicity of AgNP depends on the particle size and the amount of exposure to silver [45]. A study investigating the size of NP and their ability to accumulate in various organs has reported that the concentration of silver was significantly higher in studied organs of rats treated with 20 nm AgNP than in treated with 200 nm AgNP [46]. However, recent studies have shown that there are no detectable toxic effects of oral colloidal nano silver in humans at low plasma concentration [47–49]. A study indicates that the dose of AgNP < 10 mg/kg is safe and it has no side-effects for biomedical application, but its high dose > 20 mg/kg showed toxic effect [9].

In a previous study, the functionalization of AgNP with 5-fluorouracil was reported to increase the apoptosis induction by LDH leakage and DNA fragmentation in baby hamster kidney (BHK21) and human colon adenocarcinoma (HT29) cell lines [50].Similarly in an attempt to decrease the dose of AgNP to reduce the toxicity, we had exploited the synergism between GEM and AgNP. Surface modified drug delivery system with anticancer drug is a crucial factor to induce synergistic drug actions and reduce the toxicity of drug [11]. The beneficial effect of (GEM-AgNP) surface functionalization with anticancer drug could be attributed to stabilization of the AgNP coupled with DNA interaction and manifestation of anticancer activity through cell cycle arrest. Both GEM and AgNP exert their cytotoxic effect through DNA damage. The AgNP induces dysfunction of mitochondria by generating reactive oxygen species which causes damage to cell membranes, proteins and DNA synthesis. This results in cell cycle arrest followed by apoptosis [15,51]. GEM is a prodrug which undergoes intracellular phosphorylation to active form and gets incorporated into DNA to induce DNA damage and apoptosis [52,53]. A recent study has tested synergism between of GEM and AgNP at their respective IC_{25} values in ovarian cancer cells. Even though a synergistic action between GEM and AgNP was observed, the tested concentration of AgNP however had resulted in toxicity. The treatment was carried out as separate entities and no conjugation was done between GEM and AgNP [54].

In our study, the IC_{50} of AgNP was found to be 71.45 μg/ml (Fig. 7A), which was in close range with the previously reported IC_{50} for chemically-synthesized AgNP (72 μg/ml) [55]. The AgNP does not produce significant cytotoxicity up to 6.25 μg/ml (Fig. 7B), which confirms that the selected range of dose of AgNP was non-cytotoxic to the MDA-MB-453 cells. Previous reports have indicated that the synergistic effect could be enhanced when a drug is modified on its surface by conjugation rather than treating combination of two therapeutic agents [56,57]. Hence, we prepared the different concentrations of GEM electro statically conjugated to AgNP with a maximum of 5.45 μg/ml of AgNP. As a major observation, we found that the GEM-(non-cytotoxic AgNP) conjugates significantly increased the cytotoxicity at 12.5, 25.0 and 50.0 μM when compared to GEM alone (Fig. 7B and C). Thus, a significant improvement in cytotoxicity was achieved with non-cytotoxic AgNP concentration. Additionally, the IC_{50} value of GEM-(non-cytotoxic AgNP) (37.64 μM) was significantly lower when compared to GEM (56.54 μM) alone (Table S3).

The synergistic action of GEM-(non-cytotoxic AgNP) was confirmed using CompuSyn software (Fig. 8). The CI values of all the tested dose was < 1 which indicates the synergism between the two agents. Additionally, there is a drastic reduction of AgNP dose required to exhibit the same level of inhibition when conjugated with GEM (Table S4). According to the calculated dose reduction index (DRI), it requires 1.70-fold less GEM plus 42.55-fold less AgNP to achieve the same 50 %

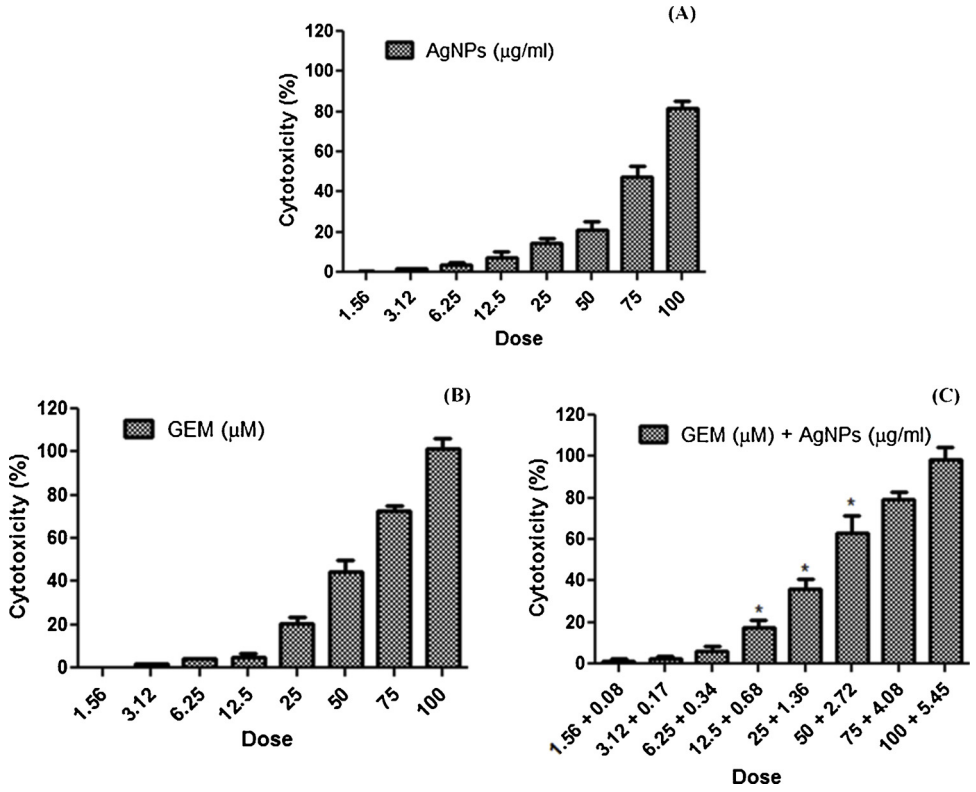

Fig. 7. Percentage inhibition of viability of MDA-MB-453 cells (A) AgNP, (B) GEM and (C) GEM-AgNP. The * indicates the significant difference in the cytotoxicity of GEM-AgNP when compared to similar doses of GEM alone. *P < 0.05.

inhibition at 18.38 (GEM): 1 (AgNP) ratio this indicates that the functionalization enhances the cytotoxic property. Functionalization refers to the surface modification of nano particles, which includes conjugation of drugs or biomolecules onto its surface. The functionalized nanoparticles have good physical and chemical properties. The effective treatment of cancer in solid tumors mainly depends on adequate delivery of the drug to the tumor cells. Typically, combination therapy gives better effect than treating drugs alone, but functionalizing therapeutic agents by conjugation gives more effect on tumor cells. This is because conjugation results in adequate delivery of both the therapeutic agents into the tumor cells. Functionalized therapeutic agents could reach the tumor cells and produces better synergistic action than when the agents were treated alone.

In this study, we have developed an electrostatic surface functionalization of GEM (positive charge) over AgNP (negative charge, non-cytotoxic dose), the resultant conjugates showed enhanced cytotoxic

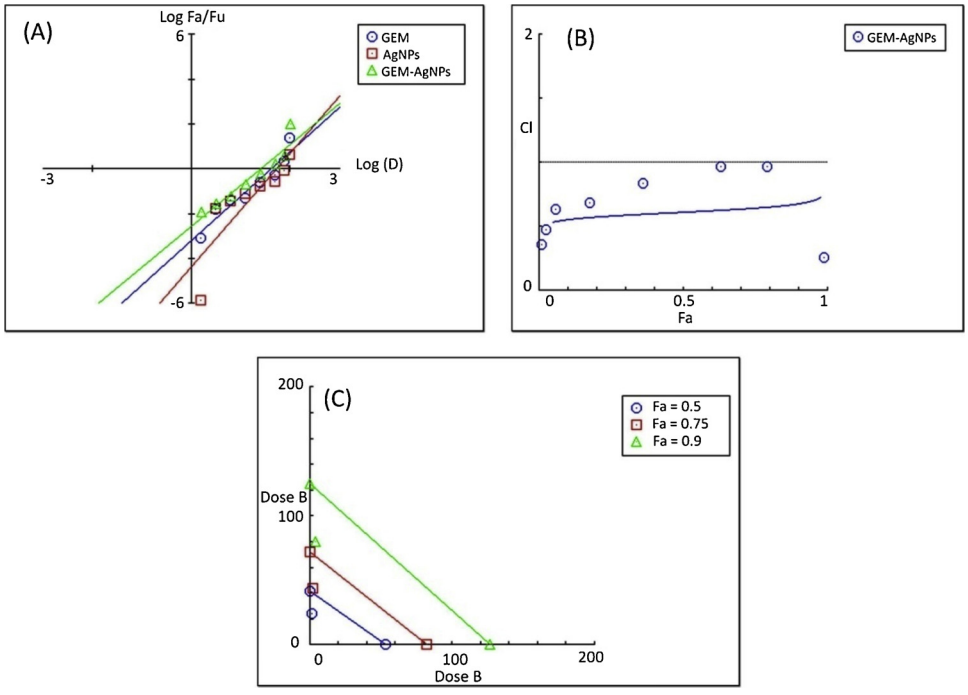

Fig. 8. The figure represents the CompuSyn Report for GEM-AgNP combinations. (A) Median-effect plot. The IC_{50} value is the anti-log of the x-axis intercept, and the m value is the slope of the plot. (B) Combination index plot. The synergy, additive and antagonistic effect of the combination are defined as CI < 1, CI = 1, and CI > 1, respectively. Among the 8 combination data points 6 of them are on the synergy side CI < 1 and 2 are nearer to additive line Cl = 1. (C) Isobolograms. Isobolograms for 50 % (Fa 0.5), 75 % (Fa 0.75), and 90 % (Fa 0.9) inhibition are shown. The data points of the combination on the diagonal line indicates additive effect, on the lower left indicates synergism, and on the upper right indicates antagonism. Here, IC_{50}, IC_{75} and IC_{90} showed synergism.

effect as compared to GEM alone. Surface electrostatic functionalization technique is simple and cost-effective method when compared to disulfide linkers, dipeptide linkers and hydrazone bonds (amine groups with covalent linker). In this work, we attempted to test how surface functionalization could increase the cytotoxicity of a cytotoxic drug (GEM) when combined with a non-cytotoxic dose of AgNP. The novelty in this work highlights specifically the evaluation of the cytotoxic effects of non-cytotoxic dose of AgNPs with Gemcitabine. The results outcome confirmed that cytotoxicity of GEM was enhanced, and synergistic effect was achieved with non-cytotoxic dose of AgNPs.

4. Conclusion

In this study, we investigated the synergism between GEM and AgNP in order to reduce the dose of AgNP and its associated toxicity. To improve the safety and efficacy of metallic nanoparticles, we used GEM as a "model" drug and prepared GEM conjugated with non-cytotoxic doses of AgNP. The stable AgNP were prepared using PVP. The prepared GEM-(non-cytotoxic AgNP) improved the cytotoxic effect of GEM in MDA-MB-453 cell line. The IC_{50} value of GEM-(non-cytotoxic AgNP) was significantly lower when compared to GEM alone. The synergism between the agents was confirmed by CompuSyn software. The GEM-(non-cytotoxic AgNP) conjugates significantly increased the cytotoxicity when compared to GEM alone. Thus, a significant improvement in cytotoxicity was achieved with non-cytotoxic AgNP concentration. Functionalization of anticancer drugs with noncytotoxic doses of AgNP could be an effective therapeutic strategy for efficacious cancer treatment. In future the obtained GEM-AgNP conjugates would be delivered to the cancer site with suitable polymeric drug delivery system.

CRediT authorship contribution statement

Arjunan Karuppaiah: Conceptualization, Methodology, Data curation, Validation, Writing - original draft. **Karthik Siram:** Software. **Divakar Selvaraj:** Software, Writing - review & editing. **Mohankandhasamy Ramasamy:** Validation, Writing - review & editing. **Dinesh Babu:** Visualization, Investigation, Writing - review & editing. **Veintramuthu Sankar:** Supervision, Investigation, Validation, Writing - review & editing.

Declaration of Competing Interest

The authors declare that there are no conflicts of interest.

Acknowledgments

The authors would like to thank Peelamedu Saamanaidu Govindaswamy (PSG) Sons & Charities for providing all the necessary research facilities. The authors also would like to thank Dr. Reddy's Laboratories Ltd. (Hyderabad, Andhra Pradesh, India) for providing gift sample of gemcitabine hydrochloride to carry out this research study. Also, we would like to thank pharmacology team, Department of Pharmacology, JSS College of Pharmacy, Tamil Nadu, India, for helping to carry out combination index studies. The authors would like to thank Department of Science and Technology – Fund for Improvement of Science and Technology Infrastructure in Universities and Higher Educational Institutions (DST-FIST), New Delhi for their infrastructure support for Department of pharmacology, JSS College of Pharmacy, Ooty. Also, we would like to thank Dr. Puthussericka A. Hassan (Scientific Officer (H) & Head, Nanotherapeutics and Biosensors Section, Chemistry Division, Bhabha Atomic Research Centre, Trombay, Mumbai – 400 085) for giving immense support and technical guidance. This work is a part of Ph.D. thesis submitted to the Tamil Nadu Dr. M.G.R. Medical University, Chennai, India.

Appendix A. Supplementary data

Supplementary material related to this article can be found, in the online version, at doi:https://doi.org/10.1016/j.mtcomm.2019.100884.

References

[1] W.H. Gmeiner, S. Ghosh, Nanotechnology for cancer treatment, Nanotechnol. Rev. 3 (2014), https://doi.org/10.1515/ntrev-2013-0013.
[2] A.R. Chowdhuri, S. Tripathy, C. Haldar, S. Chandra, B. Das, S. Roy, S.K. Sahu, Theoretical and experimental study of folic acid conjugated silver nanoparticles through electrostatic interaction for enhance antibacterial activity, RSC Adv. 5 (2015) 21515–21524, https://doi.org/10.1039/C4RA16785F.
[3] A. Sharma, A.K. Goyal, G. Rath, Recent advances in metal nanoparticles in cancer therapy, J. Drug Target. 26 (2018) 617–632, https://doi.org/10.1080/1061186X.2017.1400553.
[4] A. Yusuf, A. Brophy, B. Gorey, A. Casey, Liposomal encapsulation of silver nanoparticles enhances cytotoxicity and causes induction of reactive oxygen species-independent apoptosis, J. Appl. Toxicol. 38 (2018) 616–627, https://doi.org/10.1002/jat.3566.
[5] L. Paiva, T.K.S. Fidalgo, L.P. da Costa, L.C. Maia, L. Balan, K. Anselme, L. Ploux, R.M.S.M. Thiré, Antibacterial properties and compressive strength of new one-step preparation silver nanoparticles in glass ionomer cements (NanoAg-GIC), J. Dent. 69 (2018) 102–109, https://doi.org/10.1016/j.jdent.2017.12.003.
[6] T.Q. Huy, N.T. Hien Thanh, N.T. Thuy, P. Van Chung, P.N. Hung, A.-T. Le, N.T. Hong Hanh, Cytotoxicity and antiviral activity of electrochemical – synthesized silver nanoparticles against poliovirus, J. Virol. Methods 241 (2017) 52–57, https://doi.org/10.1016/j.jviromet.2016.12.015.
[7] D. McShan, P.C. Ray, H. Yu, Molecular toxicity mechanism of nanosilver, J. Food Drug Anal. 22 (2014) 116–127, https://doi.org/10.1016/j.jfda.2014.01.010.
[8] J.-S. Hong, S. Kim, S.H. Lee, E. Jo, B. Lee, J. Yoon, I.-C. Eom, H.-M. Kim, P. Kim, K. Choi, M.Y. Lee, Y.-R. Seo, Y. Kim, Y. Lee, J. Choi, K. Park, Combined repeated-dose toxicity study of silver nanoparticles with the reproduction/developmental toxicity screening test, Nanotoxicology 8 (2014) 349–362, https://doi.org/10.3109/17435390.2013.780108.
[9] D.K. Tiwari, T. Jin, J. Behari, Dose-dependent in-vivo toxicity assessment of silver nanoparticle in Wistar rats, Toxicol. Mech. Methods 21 (2011) 13–24, https://doi.org/10.3109/15376516.2010.529184.
[10] D. Lim, J. Roh, H. Eom, J.-Y. Choi, J. Hyun, J. Choi, Oxidative stress-related PMK-1 P38 MAPK activation as a mechanism for toxicity of silver nanoparticles to reproduction in the nematode Caenorhabditis elegans, Environ. Toxicol. Chem. 31 (2012) 585–592, https://doi.org/10.1002/etc.1706.
[11] S. Gurunathan, M.-H. Kang, M. Qasim, J.-H. Kim, Nanoparticle-mediated combination therapy: two-in-one approach for cancer, Int. J. Mol. Sci. 19 (2018) 3264, https://doi.org/10.3390/ijms19103264.
[12] D. Miles, G. von Minckwitz, A.D. Seidman, Combination versus sequential single-agent therapy in metastatic breast cancer, Oncologist 7 (Suppl 6) (2002) 13–19 http://www.ncbi.nlm.nih.gov/pubmed/12454315.
[13] J.-H. Lee, K.-J. Chen, S.-H. Noh, M.A. Garcia, H. Wang, W.-Y. Lin, H. Jeong, B.J. Kong, D.B. Stout, J. Cheon, H.-R. Tseng, On-demand drug release system for in vivo cancer treatment through self-assembled magnetic nanoparticles, Angew. Chemie Int. Ed. 52 (2013) 4384–4388, https://doi.org/10.1002/anie.201207721.
[14] A. Hekmat, A.A. Saboury, A. Divsalar, The effects of silver nanoparticles and doxorubicin combination on DNA structure and its antiproliferative effect against T47D and MCF7 cell lines, J. Biomed. Nanotechnol. 8 (2012) 968–982 http://www.ncbi.nlm.nih.gov/pubmed/23030005.
[15] M. Azizi, H. Ghourchian, F. Yazdian, S. Bagherifam, S. Bekhradnia, B. Nyström, Anti-cancerous effect of albumin coated silver nanoparticles on MDA-MB 231 human breast cancer cell line, Sci. Rep. 7 (2017) 5178, https://doi.org/10.1038/s41598-017-05461-3.
[16] K. Ranoszek-Soliwoda, E. Tomaszewska, E. Socha, P. Krzyczmonik, A. Ignaczak, P. Orlowski, M. Krzyzowska, G. Celichowski, J. Grobelny, The role of tannic acid and sodium citrate in the synthesis of silver nanoparticles, J. Nanopart. Res. 19 (2017) 273, https://doi.org/10.1007/s11051-017-3973-9.
[17] A. Mirzaei, K. Janghorban, B. Hashemi, M. Bonyani, S.G. Leonardi, G. Neri, Characterization and optical studies of PVP-capped silver nanoparticles, J. Nanostruct. Chem. 7 (2017) 37–46, https://doi.org/10.1007/s40097-016-0212-3.
[18] V. Dugandžić, I.J. Hidi, K. Weber, D. Cialla-May, J. Popp, In situ hydrazine reduced silver colloid synthesis – enhancing SERS reproducibility, Anal. Chim. Acta 946 (2016) 73–79, https://doi.org/10.1016/j.aca.2016.10.018.
[19] Z.-P. Cheng, X.-Z. Chu, X.-Q. Wu, J.-M. Xu, H. Zhong, J.-Z. Yin, Controlled synthesis of silver nanoplates and nanoparticles by reducing silver nitrate with hydroxylamine hydrochloride, Rare Met. 36 (2017) 799–805, https://doi.org/10.1007/s12598-017-0949-y.
[20] S. Iravani, H. Korbekandi, S.V. Mirmohammadi, B. Zolfaghari, Synthesis of silver nanoparticles: chemical, physical and biological methods, Res. Pharm. Sci. 9 (2019) 385–406 (n.d.), http://www.ncbi.nlm.nih.gov/pubmed/26339255.
[21] L. Mulfinger, S.D. Solomon, M. Bahadory, A.V. Jeyarajasingam, S.A. Rutkowsky, C. Boritz, Synthesis and study of silver nanoparticles, J. Chem. Educ. 84 (2007) 322, https://doi.org/10.1021/ed084p322.
[22] N. Zandi-Atashbar, B. Hemmateenejad, M. Akhond, Determination of amylose in Iranian rice by multivariate calibration of the surface plasmon resonance spectra of

silver nanoparticles, Analyst 136 (2011) 1760, https://doi.org/10.1039/c0an00863j.
[23] A. Abbaszadegan, M. Nabavizadeh, A. Gholami, Z.S. Aleyasin, S. Dorostkar, M. Saliminasab, Y. Ghasemi, B. Hemmateenejad, H. Sharghi, Positively charged imidazolium-based ionic liquid-protected silver nanoparticles: a promising disinfectant in root canal treatment, Int. Endod. J. 48 (2015) 790–800, https://doi.org/10.1111/iej.12377.
[24] R.A. Sperling, W.J. Parak, Surface modification, functionalization and bioconjugation of colloidal inorganic nanoparticles, Philos. Trans. R. Soc. A Math. Phys. Eng. Sci. 368 (2010) 1333–1383, https://doi.org/10.1098/rsta.2009.0273.
[25] V.R. Chaudhari, S.K. Haram, S.K. Kulshreshtha, J.R. Bellare, P.A. Hassan, Micelle assisted morphological evolution of silver nanoparticles, Colloids Surf. A Physicochem. Eng. Asp. 301 (2007) 475–480, https://doi.org/10.1016/j.colsurfa.2007.01.025.
[26] C. Ni, P.A. Hassan, E.W. Kaler, Structural characteristics and growth of pentagonal silver nanorods prepared by a surfactant method, Langmuir 21 (2005) 3334–3337, https://doi.org/10.1021/la046807c.
[27] S. Park, H. Chibli, J. Wong, J.L. Nadeau, Antimicrobial activity and cellular toxicity of nanoparticle–polymyxin B conjugates, Nanotechnology 22 (2011) 185101, , https://doi.org/10.1088/0957-4484/22/18/185101.
[28] G.A. Dichello, T. Fukuda, T. Maekawa, R.L.D. Whitby, S.V. Mikhalovsky, M. Alavijeh, A.S. Pannala, D.K. Sarker, Preparation of liposomes containing small gold nanoparticles using electrostatic interactions, Eur. J. Pharm. Sci. 105 (2017) 55–63, https://doi.org/10.1016/j.ejps.2017.05.001.
[29] A. Sooresh, H. Kwon, R. Taylor, P. Pietrantonio, M. Pine, C.M. Sayes, Surface functionalization of silver nanoparticles: novel applications for insect vector control, ACS Appl. Mater. Interfaces 3 (2011) 3779–3787, https://doi.org/10.1021/am201167v.
[30] N. Ivanova, V. Gugleva, M. Dobreva, I. Pehlivanov, S. Stefanov, V. Andonova, Silver nanoparticles as multi-functional drug delivery systems, Nanomedicines, IntechOpen, 2019, https://doi.org/10.5772/intechopen.80238.
[31] B. Shrestha, L. Tang, G. Romero, Nanoparticles-mediated combination therapies for cancer treatment, Adv. Ther. 2 (2019) 1900076, , https://doi.org/10.1002/adtp.201900076.
[32] H.J. Noh, A.-R. Im, H.-S. Kim, J.K. Sohng, C.-K. Kim, Y.S. Kim, S. Cho, Y. Park, Antibacterial activity and increased freeze-drying stability of sialyllactose-reduced silver nanoparticles using sucrose and trehalose, J. Nanosci. Nanotechnol. 12 (2012) 3884–3895 http://www.ncbi.nlm.nih.gov/pubmed/22852321.
[33] S. Hamarat Sanlıer, M. Yasa, A.O. Cihnioglu, M. Abdulhayoglu, H. Yılmaz, G. Ak, Development of gemcitabine-adsorbed magnetic gelatin nanoparticles for targeted drug delivery in lung cancer, Artif. Cells Nanomed. Biotechnol. (2015) 1–7, https://doi.org/10.3109/21691401.2014.1001493.
[34] V.V. Pinto, M.J. Ferreira, R. Silva, H.A. Santos, F. Silva, C.M. Pereira, Long time effect on the stability of silver nanoparticles in aqueous medium: effect of the synthesis and storage conditions, Colloids Surf. A Physicochem. Eng. Asp. 364 (2010) 19–25, https://doi.org/10.1016/j.colsurfa.2010.04.015.
[35] I.V. Bijnsdorp, E. Giovannetti, G.J. Peters, Analysis of Drug Interactions, (2011), pp. 421–434, https://doi.org/10.1007/978-1-61779-080-5_34.
[36] A. Zielińska, E. Skwarek, A. Zaleska, M. Gazda, J. Hupka, Preparation of silver nanoparticles with controlled particle size, Procedia Chem. 1 (2009) 1560–1566, https://doi.org/10.1016/j.proche.2009.11.004.
[37] B. Yahyaei, P. Pourali, One step conjugation of some chemotherapeutic drugs to the biologically produced gold nanoparticles and assessment of their anticancer effects, Sci. Rep. 9 (2019) 10242, https://doi.org/10.1038/s41598-019-46602-0.
[38] L. Jiang, M. Krasowska, D. Fornasiero, P. Koh, J. Ralston, Electrostatic attraction between a hydrophilic solid and a bubble, Phys. Chem. Chem. Phys. 12 (2010) 14527, https://doi.org/10.1039/c0cp01367f.
[39] S. Karthik, C.V. Raghavan, G. Marslin, H. Rahman, D. Selvaraj, K. Balakumar, G. Franklin, Quillaja saponin: a prospective emulsifier for the preparation of solid lipid nanoparticles, Colloids Surf. B Biointerfaces 147 (2016) 274–280, https://doi.org/10.1016/j.colsurfb.2016.07.065.
[40] J.D. Clogston, A.K. Patri, Zeta Potential Measurement, (2011), pp. 63–70, https://doi.org/10.1007/978-1-60327-198-1_6.
[41] I. Sondi, B. Salopek-Sondi, Silver nanoparticles as antimicrobial agent: a case study on E. coli as a model for gram-negative bacteria, J. Colloid Interface Sci. 275 (2004) 177–182, https://doi.org/10.1016/j.jcis.2004.02.012.
[42] Y. Han, W. Liu, J. Huang, S. Qiu, H. Zhong, D. Liu, J. Liu, Cyclodextrin-based metal-organic frameworks (CD-MOFs) in pharmaceutics and biomedicine, Pharmaceutics 10 (2018) 271, https://doi.org/10.3390/pharmaceutics10040271.
[43] H. Moradi-Sardareh, H.R.G. Basir, Z.M. Hassan, M. Davoudi, F. Amidi, M. Paknejad, Toxicity of silver nanoparticles on different tissues of Balb/C mice, Life Sci. 211 (2018) 81–90, https://doi.org/10.1016/j.lfs.2018.09.001.
[44] J.S. Teodoro, A.M. Simões, F.V. Duarte, A.P. Rolo, R.C. Murdoch, S.M. Hussain, C.M. Palmeira, Assessment of the toxicity of silver nanoparticles in vitro: a mitochondrial perspective, Toxicol. In Vitro 25 (2011) 664–670, https://doi.org/10.1016/j.tiv.2011.01.004.
[45] C. Recordati, M. De Maglie, S. Bianchessi, S. Argentiere, C. Cella, S. Mattiello, F. Cubadda, F. Aureli, M. D'Amato, A. Raggi, C. Lenardi, P. Milani, E. Scanziani, Tissue distribution and acute toxicity of silver after single intravenous administration in mice: nano-specific and size-dependent effects, Part. Fibre Toxicol. 13 (2015) 12, https://doi.org/10.1186/s12989-016-0124-x.
[46] K. Dziendzikowska, J. Gromadzka-Ostrowska, A. Lankoff, M. Oczkowski, A. Krawczyńska, J. Chwastowska, M. Sadowska-Bratek, E. Chajduk, M. Wojewódzka, M. Dušinská, M. Kruszewski, Time-dependent biodistribution and excretion of silver nanoparticles in male Wistar rats, J. Appl. Toxicol. 32 (2012) 920–928, https://doi.org/10.1002/jat.2758.
[47] M.A. Munger, G. Hadlock, G. Stoddard, M.H. Slawson, D.G. Wilkins, N. Cox, D. Rollins, Assessing orally bioavailable commercial silver nanoparticle product on human cytochrome P450 enzyme activity, Nanotoxicology 9 (2015) 474–481, https://doi.org/10.3109/17435390.2014.948092.
[48] K.J. Smock, R.L. Schmidt, G. Hadlock, G. Stoddard, D.W. Grainger, M.A. Munger, Assessment of orally dosed commercial silver nanoparticles on human ex vivo platelet aggregation, Nanotoxicology 8 (2014) 328–333, https://doi.org/10.3109/17435390.2013.788749.
[49] X.-F. Zhang, Z.-G. Liu, W. Shen, S. Gurunathan, Silver nanoparticles: synthesis, characterization, properties, applications, and therapeutic approaches, Int. J. Mol. Sci. 17 (2016) 1534, https://doi.org/10.3390/ijms17091534.
[50] P. Gopinath, S.K. Gogoi, A. Chattopadhyay, S.S. Ghosh, Implications of silver nanoparticle induced cell apoptosis for in vitro gene therapy, Nanotechnology 19 (2008) 075104, , https://doi.org/10.1088/0957-4484/19/7/075104.
[51] A. El-Hussein, M.R. Hamblin, ROS generation and DNA damage with photo-inactivation mediated by silver nanoparticles in lung cancer cell line, IET Nanobiotechnol. 11 (2017) 173–178, https://doi.org/10.1049/iet-nbt.2015.0083.
[52] R.-R. Zheng, W. Hu, C.-G. Sui, N. Ma, Y.-H. Jiang, Effects of doxorubicin and gemcitabine on the induction of apoptosis in breast cancer cells, Oncol. Rep. 32 (2014) 2719–2725, https://doi.org/10.3892/or.2014.3513.
[53] S. Wu, J. Guo, W. Wei, J. Zhang, J. Fang, S.J. Beebe, Enhanced breast cancer therapy with nsPEFs and low concentrations of gemcitabine, Cancer Cell Int. 14 (2014) 98, https://doi.org/10.1186/s12935-014-0098-4.
[54] G.S. Yuan, Peng YG, QL, Silver nanoparticles enhance the apoptotic potential of gemcitabine in human ovarian cancer cells: combination therapy for effective cancer treatment, Int. J. Nanomed. 5 (2017) 6487–6502.
[55] D. Solairaj, P. Rameshthangam, G. Arunachalam, Anticancer activity of silver and copper embedded chitin nanocomposites against human breast cancer (MCF-7) cells, Int. J. Biol. Macromol. 105 (2017) 608–619, https://doi.org/10.1016/j.ijbiomac.2017.07.078.
[56] R. Thiruppathi, S. Mishra, M. Ganapathy, P. Padmanabhan, B. Gulyás, Nanoparticle functionalization and its potentials for molecular imaging, Adv. Sci. 4 (2017) 1600279, , https://doi.org/10.1002/advs.201600279.
[57] M.M. Lin, H.-H. Kim, H. Kim, J. Dobson, D.K. Kim, Surface activation and targeting strategies of superparamagnetic iron oxide nanoparticles in cancer-oriented diagnosis and therapy, Nanomedicine 5 (2010) 109–133, https://doi.org/10.2217/nnm.09.96.